182 7/14/80 T. S.

I - 11187

SAND80-0432
Unlimited Release
UC-79c

MASTER

Calculation of the Response of Cylindrical Targets to Collimated Beams of Particles Using One-Dimensional Adjoint Transport Techniques

Stephen A. Dupree

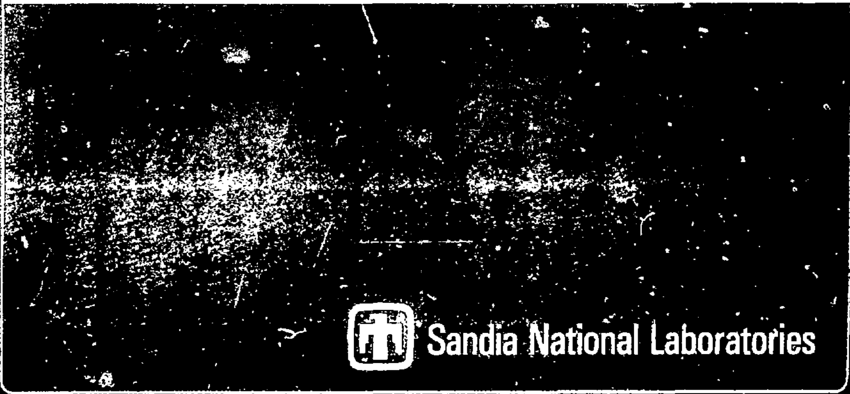

SF 2900-Q(3-80)

SAND80-0432
Unlimited Release
Printed June 1980

Distribution
Category UC-79c

CALCULATION OF THE RESPONSE OF CYLINDRICAL TARGETS TO COLLIMATED BEAMS OF PARTICLES USING ONE-DIMENSIONAL ADJOINT TRANSPORT TECHNIQU

Stephen A. Dupree
Theoretical Division 4231
Sandia National Laboratories
Albuquerque, NM 87185

ABSTRACT

The use of adjoint techniques to determine the interaction of externally incident collimated beams of particles with cylindrical targets is a convenient means of examining a class of problems important in radiation transport studies. The theory relevant to such applications is derived, and a simple example involving a fissioning target is discussed. Results from both discrete ordinates and Monte Carlo transport-code calculations are presented, and comparisons are made with results obtained from forward calculations. The accuracy of the discrete ordinates adjoint results depends on the order of angular quadrature used in the calculation. Reasonable accuracy by using EQN quadratures can be expected from order S_{16} or higher.

CONTENTS

ILLUSTRATIONS

TABLES

CALCULATION OF THE RESPONSE OF CYLINDRICAL TARGETS TO COLLIMATED BEAMS OF PARTICLES USING ONE-DIMENSIONAL ADJOINT TRANSPORT TECHNIQUES

Introduction

A problem frequently encountered in radiation transport studies involves the response of a target to a collimated beam of incident particles. This type of problem typically requires calculation of the number of reactions of a given type that occur in specific regions of the target per unit incident beam fluence. Such problems are readily amenable to the use of adjoint transport calculations.

The use of adjoint calculations to obtain neutron penetration factors in spherical geometry has been described by Hansen and Sandmeier.[1] Numerous applications of this technique in spherical and slab geometry, using both discrete ordinates and Monte Carlo transport codes, have been published (e.g., see References 2, 3, and 4). The purpose of the present paper is to extend the adjoint technique of Hansen and Sandmeier to cylindrical geometry and to present the results of a simple cylindrical test problem. As in previous studies, the principal motivation behind the use of adjoint as opposed to forward techniques to solve this type of problem is the saving of computer time achieved; i.e., one forward calculation *must be performed for each incident-particle energy in order to obtain the information* produced in a single adjoint calculation.

Theory

The forward and adjoint steady-state transport equations may be written as

$$\bar{\Omega} \cdot \bar{\nabla}\phi + \Sigma^t\phi = \int \phi\Sigma^s(E'\rightarrow E,\ \bar{\Omega}'\rightarrow\bar{\Omega})\ dE' d\bar{\Omega}' + S\ , \tag{1}$$

and

$$-\bar{\Omega} \cdot \bar{\nabla}\phi^+ + \Sigma^t\phi^+ = \int \phi^+\Sigma^s(E\rightarrow E',\ \bar{\Omega}\rightarrow\bar{\Omega}')\ dE'\ d\bar{\Omega}' + S^+\ , \tag{2}$$

respectively. The present notation is similar to that of Hansen and Sandmeier.[1] The particle flux ϕ (adjoint flux ϕ^+) is a function of space, energy, and angle $(\bar{r},\ E,\ \bar{\Omega})$; the source S (adjoint source S^+) is a function of $(\bar{r}, E)$. Multiplying Eq. (1) by ϕ^+ and Eq. (2) by ϕ, subtracting the products, and integrating over the relevant ranges of E and $\bar{\Omega}$, and over the volume of a region of interest V, gives*

---

*Details of the derivation of this result have been presented elsewhere; see, for example, References 1 and 2.

$$\iiint_{V\bar{\Omega}E} \phi S^{+}\, dE\, d\bar{\Omega}\, dV = \iiint_{V\bar{\Omega}E} \phi^{+} S\, dE\, d\bar{\Omega}\, dV$$

$$+ \iiint_{\bar{\Omega}EA} \phi\phi^{+} (\bar{\Omega} \cdot \bar{n})\, dA\, dE\, d\bar{\Omega} \quad . \tag{3}$$

Here $\bar{n}$ is the unit inner normal on the surface A bounding the volume V. The surface A is assumed to consist of the points $\bar{r}_A$.

Eq. (3) may be used to relate the adjoint source and flux to the physical quantities of interest by judicious definition of S, S^{+}, and A. Specifically, the response of a target to a particle beam may be obtained by defining $S^{+}(\bar{r},E) = \Sigma(\bar{r},E)$, where Σ is a reaction cross section of interest and $S = 0$. In this case Eq. (3) becomes

$$R = \iiint_{V\bar{\Omega}E} \phi\Sigma\, dE\, d\bar{\Omega}\, dV = \iiint_{\bar{\Omega}EA} \phi\phi^{+} (\bar{\Omega} \cdot \bar{n})\, dA\, dE\, d\bar{\Omega} \ , \tag{4}$$

where R is the number of reactions of the type defined by Σ that occur inside the volume V due to the forward particle flux ϕ. The importance of this result is that, using Eq. (4), R may be determined by the integral on the right for which ϕ need be known only on the surface A.

To cast Eq. (4) into cylindrical geometry, consider Figure 1. In this geometry a parallel beam of particles, moving in direction $\bar{\Omega}$ (the -x direction in the figure), is assumed incident on an infinite cylinder oriented normal to the beam. The volume V is defined as the interior of the cylinder, which is bounded by the surface A of radius r_A. The forward flux ϕ on the surface A is given by

$$\phi = S_o(E)\ \delta\ (\bar{\Omega} - \bar{\Omega}_o) \ . \tag{5}$$

On the surface A the adjoint flux depends on $\bar{\Omega}_o$ and $\bar{r}_A$ through the scalar product

$$\mu = \bar{\Omega}_o \cdot \bar{n} = \cos\theta \ ,$$

where θ is the azimuthal angle shown in Figure 1.
The surface differential*

$$dA = 2r_A\, d\theta\, dz \ ,$$

*The factor of 2 in the expression for dA accounts for the symmetry about $\theta = 0$.

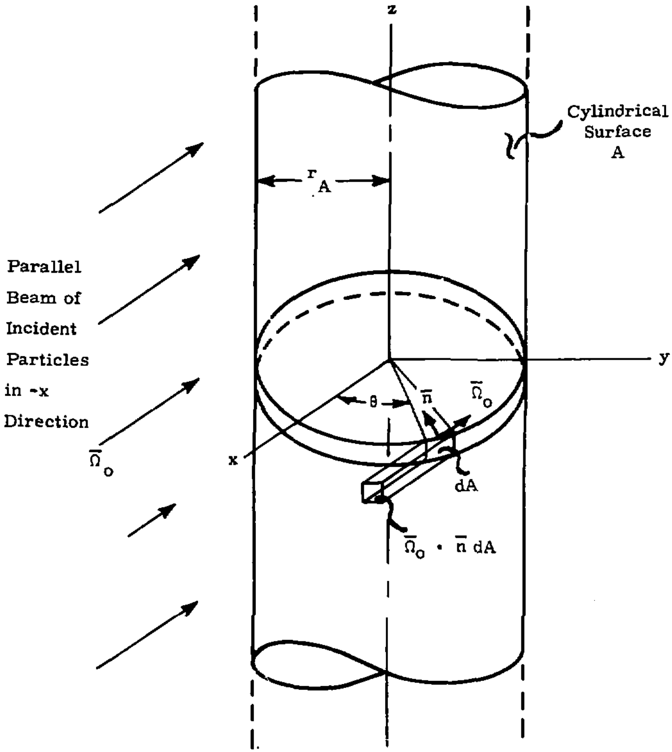

Figure 1. Geometry for Cylindrical Adjoint Calculations

projected along the incident particle direction, is

$$\bar{\Omega}_o \cdot \bar{n}\, dA = \frac{-2r_A \mu d\mu\, dz}{\sqrt{1 - \mu^2}} . \tag{6}$$

Substituting Eqs. (5) and (6) into Eq. (4) gives

$$R = -2r_A \iint \frac{S_o(E)\ \phi^+ \mu}{\sqrt{1 - \mu^2}}\, d\mu\, dE , \tag{7}$$

where all quantities have been assumed independent of z and the result now refers to a unit height of the cylinder. In this equation, the angular integral is non-zero for $\mu < 0$ only since the boundary condition on ϕ^+ is $\phi^+(r_A,E,\mu) = 0$ for $\mu > 0$. Thus, by symmetry, the integral need be taken only over $0 \leq \theta \leq \pi/2$, i.e., over one-half the side of the cylinder facing the incident beam. In this case, Eq. (7) becomes

$$R = 2r_A \int_o^\infty dE\ S_o(E) \int_o^1 d\mu \frac{\phi^+ \mu}{\sqrt{1 - \mu^2}} . \tag{8}$$

One-dimensional discrete ordinate codes are well suited for solving problems of the present type. In cylindrical geometry, the angular quadrature consists of discrete directions $\bar{\Omega}_m$ as shown in Figure 2. Each discrete direction has a solid angle, or weight w_m, associated with it. There are two components of $\bar{\Omega}_m$, ξ_m, and ψ_m:

$$\mu_m = (1 - \xi_m^2)^{1/2} \cos \psi_m$$

$$\eta_m = (1 - \xi_m^2)^{1/2} \sin \psi_m , \tag{9}$$

where the (μ,η,ξ) are defined along orthogonal coordinates with unit vectors $(\hat{r},\hat{\theta},\hat{z})$ as shown in Figure 2 and $\mu_m{}^2 + \eta_m{}^2 + \xi_m{}^2 = 1$.

The $\bar{\Omega}_m$ are arranged in levels corresponding to each ξ_m. The level with ξ_m closest to zero (call it ξ_o) lies most nearly perpendicular to the z-axis and therefore corresponds closest to the direction of the collimated beam of Figure 1. For example, the quadrature directions for an S_8 EQN cylindrical quadrature in the positive (μ,η,ξ) octant are shown in Figure 3. The $\bar{\Omega}_m$ shown are numbered in the sequence required as input to ANISN. The coordinates for each $\bar{\Omega}_m$ in this quadrature set are shown to three significant figures in Table 1 (see, for example, References 5 and 6). In this set $\xi_o = 0.218...$

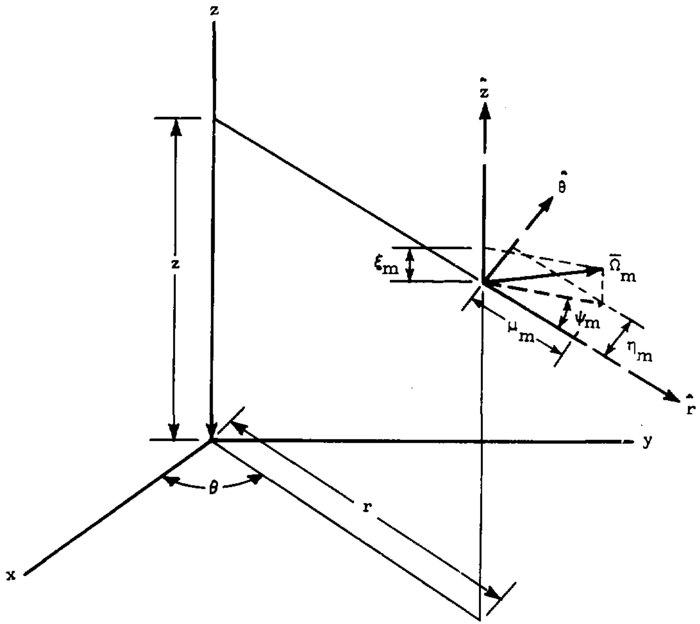

Figure 2. Discrete Directions $\bar{\Omega}_m$ in Cylindrical Geometry

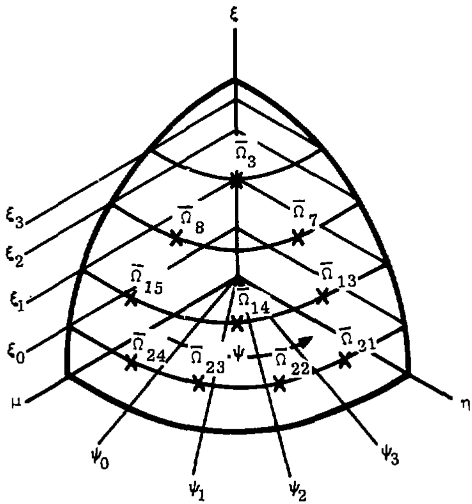

Figure 3. Discrete Angular Mesh for One Octant of an S_8 Cylindrical EQN Quadrature

In discrete ordinates, the angular integral of Eq. (8) corresponds to a summation over the leakage in the ξ_o level.* This sum is analogous to the spherical geometry result of Hansen and Sandmeier except for the consideration of the ξ_m levels in the cylindrical quadrature. Thus, ϕ^+ may be related to $L^+_{g,m}$, the angular leakage in group g and quadrature direction m, obtained in an adjoint S_n calculation for which the geometry and source correspond to the problem to be solved.

TABLE 1

Discrete Directions in
S_8 Cylindrical EQN Quadrature

m	μ	η	ξ
3	0.218	0.218	0.951
7	0.218	0.577	0.787
8	0.577	0.218	0.787
13	0.218	0.787	0.577
14	0.577	0.577	0.577
15	0.787	0.218	0.577
21	0.218	0.951	0.218
22	0.577	0.787	0.218
23	0.787	0.577	0.218
24	0.951	0.218	0.218

For a multigroup adjoint calculation, the total response R may be conveniently defined by a sum over the response in each group g,

$$R = \sum_{g=1}^{G} S_g R_g \ ,$$

where G is the number of energy groups in the calculation. In discrete notation, the angular integral of Eq. (8) may then be written**

$$R_g = r_A \sum_{\substack{m\epsilon\xi_o \\ \mu_m<0}} \frac{L^+_{g,m}\ \mu_m w'_m}{\sqrt{1-\mu_m^2}} \qquad (10)$$

*This is exact only when $\xi_o = 0$. For EQN quadratures, $\xi_o \rightarrow 0$ as the order $n \rightarrow \infty$; therefore, the accuracy of the following analysis would be expected to improve with increasing n when such quadratures are used.

**Note that, for adjoint calculations, the discrete ordinate transport codes invert the order of the energy groups but not the discrete directions. Thus, to interpret adjoint angular fluxes, the code user must correct both the groups and the angles, i.e., group G is actually group 1, and direction μ_m is actually direction $-\mu_m$.

where

$$w'_m = \frac{w_m}{\sum\limits_{\substack{k \in \xi_o \\ \mu_k < 0}} w_k} \tag{11}$$

In discrete ordinates codes the weights are normalized to unity. Thus the w_m for $m \in \xi_o$ must be normalized, as in Eq. (11), to make the discrete summation equivalent to the angular integral of Eq. (8). The factor of 2 in Eq. (8) has been omitted from Eq. (10) because the $L^+_{g,m}$ already contain the sum of the right- and left-hand azimuthal components of the angular leakage for a given ψ_m in Eq. (9).

Unlike the spherical result of Hansen and Sandmeier, the cylindrical response is not automatically calculated by the discrete ordinates transport codes. However, by printing the angular flux, the user can obtain the $L^+_{g,m}$ and perform the summation of Eq. (10) by hand. Alternatively, a simple update to the code will permit the response to be printed directly.

Example Problem

As a practical application of the cylindrical adjoint technique developed in the previous section, consider the model target system shown in Figure 4 struck by a collimated beam of neutrons. This target consists of an annulus of ^{239}Pu, 0.05 cm thick, surrounded by 1.95 cm of CH_2. The inner diameter of the ^{239}Pu annulus is 10 cm. The atomic densities of the materials, shown in Table 2, are identical to those used in the spherical fission detector example presented by Hansen and Sandmeier. Also, as in their example, the 16-group Hansen and Roach[7] neutron cross sections have been used, with P_1 scattering for H and P_0 scattering for C and ^{239}Pu.

TABLE 2

Geometry of the Cylindrical Target

Region	Material	Atom Density (10^{24} nuclei/cm^3)	Outer Radius (cm)	Number of Spatial Intervals Used in S_n Calculations
1	Void	0	5	5
2	^{239}Pu	0.0498	5.05	5
3	CH_2	N_C = 0.03957	7	20
		N_H = 0.07914		

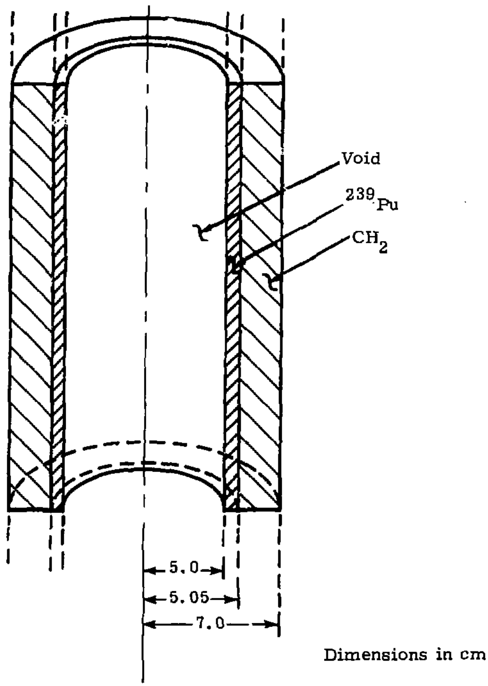

Figure 4. Geometry of Example Problem, One-Dimensional Infinite Cylinder

To determine the number of fissions induced in the ^{239}Pu of Figure 4 per incident neutron/cm^2, the adjoint source was set to $\Sigma^f(E)$, the macroscopic fission cross section of ^{239}Pu. The resulting source in the 16-group cross-section structure is shown on the left side of Table 3. With this source, the ANISN discrete ordinates transport code[6,8] was used in the adjoint mode to determine $L^+_{g,m}$, and hence the group-dependent response of Eq. (10). The results for R_g, obtained by using S_8, S_{12}, and S_{16} symmetric EQN cylindrical quadratures, are shown in the central section of Table 3.

As in spherical geometry,[1] the adjoint cylindrical geometry results can be verified with forward calculations. In this case, an angular-dependent boundary source must be used to simulate a parallel-beam source normal to the axis of the cylinder, i.e., a source is used that is constant in the angles $m\epsilon\xi_o$ and zero for all other angles. This source must be placed at a distance $r_S > \sim 5r_A$ in order to simulate a parallel beam with reasonable accuracy.[1,9] To normalize to a unit incident fluence on the cylindrical target, the forward source $S_{g,m}$ must be of magnitude

$$S_{g,m} = \left[2\sum_{m\epsilon\xi_o} w_m\right]^{-1} .$$

The discrete ordinates codes customarily contain the fission cross section only as the product $\nu\Sigma^f$. Thus, to obtain the fission response from a forward calculation with a source in group g the explicit sum

$$R_g = \sum_{i=I_1}^{I_2} \sum_{g'=1}^{G} \phi_{i,g'} \Sigma^f_{g'} \quad V_i$$

must be taken, where the sum over i refers to the pertinent spatial intervals* in the problem, and $\phi_{i,g}$ is the scalar flux. This sum is readily obtained using the activity option in discrete ordinates codes. Alternatively, the fission source calculated by the code (which is actually the fission neutron production rate) can be divided by the average number of prompt neutrons per fission to obtain R_g.

The results of S_{16} forward ANISN calculations of the fission response of the cylindrical target of Figure 3 to incident neutron beams in energy groups 1, 6, and 13 are also shown in the central section of Table 3. Obviously a forward calculation must be performed for each energy group of incident neutrons in order to duplicate the data obtained from a single adjoint calculation.

Monte Carlo adjoint calculations of the fission response of the example target to incident parallel beams of neutrons were performed with the MORSE code.[10]

*The sum need not include every interval containing fissile material; i.e., *the response can be determined as a function of space point if desired.*

TABLE 3

Results of Calculations of the Fission Response R_g *for the* Cylindrical Example Problem

Cross-Section Data			R_g, Fissions/cm per Incident Neutron/cm^2 in Group g						
			Discrete Ordinates Results				Monte Carlo Results		
			Adjoint Calculations				Adjoint Calculations		
Energy Group g	Upper Energy Bound	Adjoint Source $\Sigma^f(^{239}Pu)$	S_8	S_{12}	S_{16}	Forward Calculation	Leakage	Point Detector	Forward Calculation
1	∞	0.0946	0.35	0.40	0.45	0.54	0.54 (0.08)*	0.52 (0.05)	0.52 (0.02)
2	3.0 MeV	0.0971	0.51	0.58	0.66	-	0.89 (0.11)	0.82 (0.06)	-
3	1.4	0.0911	0.73	0.85	0.95	-	1.2 (0.11)	1.04 (0.05)	-
4	0.9	0.0846	0.94	1.09	1.22	-	1.4 (0.10)	1.33 (0.05)	-
5	0.4	0.0831	1.27	1.48	1.66	-	2.1 (0.10)	1.74 (0.06)	-
6	100 keV	0.0956	1.60	1.88	2.09	2.42	2.1 (0.10)	2.0 (0.07)	2.35 (0.01)
7	17	0.1245	1.87	2.21	2.43	-	2.3 (0.10)	2.0 (0.07)	-
8	3	0.2091	2.14	2.53	2.77	-	3.8 (0.14)	2.3 (0.08)	-
9	550 eV	0.8217	2.40	2.83	3.10	-	3.7 (0.14)	2.3 (0.08)	-
10	100	2.091	2.60	3.08	3.36	-	3.8 (0.11)	2.6 (0.10)	-
11	30	3.884	2.71	3.22	3.51	-	3.9 (0.12)	2.7 (0.11)	-
12	10	1.195	2.73	3.24	3.52	-	4.8 (0.16)	2.8 (0.12)	-
13	3	0.996	2.78	3.30	3.59	3.86	4.1 (0.18)	2.9 (0.16)	4.02 (0.01)
14	1.0	6.922	2.70	3.2[illegible]	3.51	-	4.3 (0.17)	3.0 (0.16)	
15	0.4	60.805	2.17	2.59	2.82	-	3.9 (0.19)	2.5 (0.18)	
16	0.1 (thermal)	35.109	1.25	1.50	1.63	-	1.8 (0.20)	2.3 (0.27)	

*Quantities in parentheses are the fractional standard deviation estimates.

The results from such calculations can be scored in a variety of ways. A direct analog of the discrete ordinates solution can be obtained by tallying the adjoint particles leaking from the cylinder, weighted by $\mu/\sqrt{1-\mu^2}$, as a function of energy and of angle with respect to the z-axis. Alternatively, a last-flight estimator can be used to score the adjoint flux at a distant point.*

The geometry used in the present MORSE calculations is shown in Figure 5. *Albedo media with specular reflection were used to simulate an infinite cylinder.* Proper normalization of the results requires consideration of the manner in which MORSE normalizes adjoint calculations,[10] i.e., of the fact that the result must be normalized to the total adjoint source per unit height of the cylinder. In the present case this is given by

$$V_{Pu} \sum_{g=1}^{G} \Sigma_g^f ,$$

where V_{Pu} is the volume of ^{239}Pu per unit height of the cylinder. In addition, if the direct S_n analog scoring of the adjoint leakage as a function of angle is used (along with the default angular-dependent printout) to obtain R_g, the units of this printout must be considered--viz., particles/steradian/eV. The coupling of the forward and adjoint fluxes on the surface of the cylinder in Eq. (10) then requires that the adjoint leakage be multiplied by 2π. If the distant point detector option is used to score the adjoint leakage, with the detector at a distance r_d, a factor of $4\pi r_d^2$ must be used instead.

The results of MORSE adjoint calculations for R_g, using the geometry of Figure 5, are shown on the right side of Table 3. Results for both the analog-leakage and the distant point detector tallies are shown. The point detector has the virtue of ease of use; otherwise the detectors are comparable.** The results of forward MORSE calculations for source groups 1, 6, and 13, using exactly parallel beam sources, are also shown on the right side of Table 3.

Comparisons between the results of Table 3 show general agreement for the responses R_g among the various calculations. As expected, the discrete ordinates adjoint results are sensitive to quadrature order. Figure 6 shows the ANISN results for groups 1, 6, and 13, as a function of the quadrature order n. For comparison, the ANISN and MORSE (with one standard deviation uncertainty indicated)

*There is no direct analogy in discrete ordinates to the latter scoring although a similar approach would be to surround the discrete ordinates target cylinder with a large void region. In this case the angular leakage through the outer boundary would be only in the most outward-directed μ_m direction; however, EQN quadratures do not calculate radial streaming correctly, and results obtained with such sets would be inaccurate.

**For the simple biasing scheme (source biasing and radial path stretching) used in the present calculations, a smaller variance was obtained in the high-energy groups than in the low-energy groups. The results for the low-energy groups could have been improved by the use of energy biasing; however, this was not considered necessary for the present comparison.

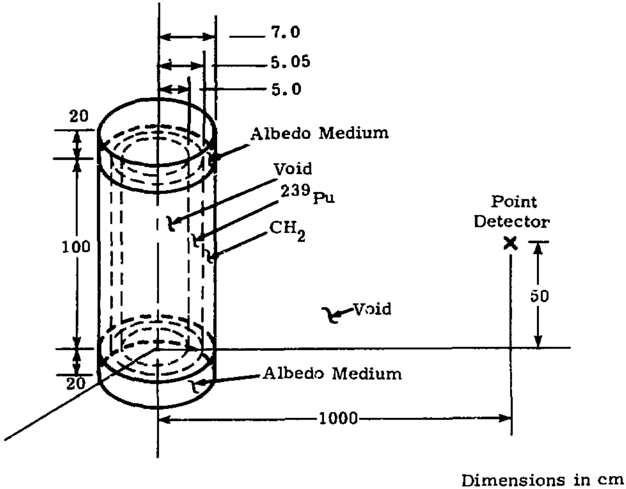

Figure 5. MORSE Geometry for Cylindrical Example Problem

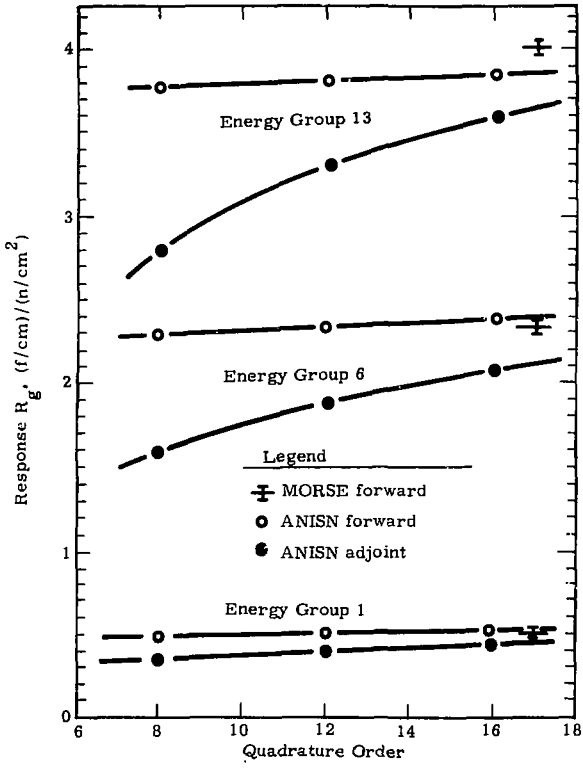

Figure 6. Comparison of Responses R_g Calculated with ANISN and MORSE

forward results for these groups are also shown. In each case the series of S_n adjoint results for increasing n approachs the MORSE results. The S_{16} results are within 10% of the MORSE results for each case; however, the S_8 results are low by about 30%. Clearly a relatively high-order EQN quadrature must be used in the type of discrete-ordinates cylindrical adjoint calculation under discussion in order to achieve a reasonable degree of accuracy in the answer. On the other hand, the upper curves for each group in Figure 6 show that the results of the forward ANISN calculations are not sensitive to quadrature order.

Apart from quadrature order, there are several differences in the various calculations that account for the lack of exact agreement among the results. Since the same cross sections were used in all of the calculations, errors in these cross sections are not of concern in this comparison. The forward MORSE results may be assumed "exact" within statistics. All the other calculations contain errors associated with the discrete angular mesh and/or the lack of exact parallelism in the beam because of a finite distance between the source and the target. Therefore, precise agreement should not be expected.

Conclusions

The cylindrical adjoint transport technique of calculating the response of a target to an incident parallel beam of particles is expected to be useful in analyzing certain problems involving targets with large length-to-diameter aspect ratios. The example presented above shows several means of obtaining response functions for such targets, all of which give reasonably accurate results provided a relatively high order of angular resolution ($\geq S_{16}$ for discrete ordinates with EQN quadratures) is used.

References

[1] G. E. Hansen and H. A. Sandmeier, "Neutron Penetration Factors Obtained by Using Adjoint Transport Calculations," Nucl Sci Eng 22, 315 (1965).

[2] J. H. Renken, Use of Solutions to the Adjoint Transport Equation for the Evaluation of Radiation Shield Designs, SC-RR-70-98 (Albuquerque: Sandia Laboratories, January 1972).

[3] W. H. Scott, Jr. et al, "Multigroup Analysis of Neutron and Secondary Gamma Ray Transport in Concrete," DNA 2994F (La Jolla, CA: Science Applications, Inc., December 1972).

[4] J. H. Renken, "Comparison of Predicted Signals from the Delayed Fission Neutron and Prompt Fission Neutron Uranium Logging Methods," J Appl Phys 49, 6153 (December 1978).

[5] K. D. Lathrop and B. G. Carlson, Discrete Ordinates Angular Quadrature of the Neutron Transport Equation, LA-3186 (Los Alamos: Los Alamos Scientific Laboratory, February 1965).

[6] R. G. Soltesz and R. K. Disney, "One-Dimensional Discrete Ordinates Transport Technique," Nuclear Rocket Shielding Methods, Modification, Updating, and Input Data Preparation, vol 4, WANL-PR-(LL)-034 (Pittsburgh: Westinghouse Astronuclear Laboratory, August 1970).

[7] G. E. Hansen and W. H. Roach, Six and Sixteen Group Cross Sections for Fast and Intermediate Critical Assemblies, LAMS-2543 (Los Alamos: Los Alamos Scientific Laboratory, December 1961).

[8] W. W. Engle, Jr., A Users Manual for ANISN, K-1693 (Oak Ridge: Union Carbide Corp. Nuclear Division, 1967).

[9] R. L. Berger and H. A. Sandmeier, Various Methods of Calculating Fission Heating in a Small Plutonium Ball Due to a Collimated Incident Neutron Beam, NWEF 1012 (Albuquerque: Naval Weapons Evaluation Facility, May 1967).

[10] S. A. Dupree and R. E. Lighthill, Sandia Laboratories' CDC7600 Version of MORSE-SGC (Albuquerque: Sandia Laboratories, to be published).